Lim, I. L. H. and Yang, D. (2017) Low-Cost Precision Motion Control for Industrial Digital Microscopy. In: 43rd Annual Conference of the IEEE Industrial Electronics Society (IES), Beijing, China, 29 Oct - 01 Nov 2017, pp. 7281-7287. ISBN 9781538611272 (doi:10.1109/IECON.2017.8217275)

This is the author's final accepted version.

There may be differences between this version and the published version. You are advised to consult the publisher's version if you wish to cite from it.

http://eprints.gla.ac.uk/163101/

Deposited on: 16 October 2017

# Low-cost Precision Motion Control for Industrial Digital Microscopy

Idris Li Hong Lim
Department of Electronic Systems
University of Glasgow
Glasgow G12 8QQ, UK
Email: LiHonIdris.Lim@glasgow.ac.uk

Dazhi Yang
Singapore Institute of
Manufacturing Technology
71 Nanyang Drive
Singapore 638705

*Abstract*—This paper presents a reliable but low-cost way for industrial digital microscopy to implement $\mu$m-level precision of X/Y stage motion control. Other than the prevailing designs using stepper motors with open-loop control algorithms, the proposed method uses DC motors with closed-loop sliding mode control (SMC) to save the cost and allow a smooth switching between manual and motorized mode for stage movement. Boundary layer (saturator) method is then applied to alleviate the chattering cause by SMC, and its accuracy loss is completely eliminated by a simple position fine-tune trick to limit the error within $\pm 2$ $\mu$m. Comparing with the main stream $\mu$m-level industrial microscopies with stepper motors, the proposed solution achieves similar performance with almost half costs.

## I. INTRODUCTION

With the rapid development of optics and zoom design, the magnification of modern industrial microscopies can be up to $2350\times$, which requires the $\mu$m-level precision of X/Y stage movement. For such a high resolution, stepper motors are usually used due to their precise structure and simplicity in control (open-loop). Consequently, the cost for the whole positioning solution is high. The main drawback of stepper motor is that shaft rotation is not allowed when power off, which means that users cannot switch smoothly between manual and motorized mode for the stage movement. While in most of applications, manual mode is still preferred by users because it brings convenience in their daily work.

One way to keep manual mode for stage movement is to use DC motor, which can also greatly reduce the cost. However, very few products in the market use DC motors except DVM6 from Leica Microsystems, which utilizes friction as the engagement between motor shaft and stage tracks to allow smooth and free switching between manual and motorized mode [1]. Due to the presence of friction, DC motor control becomes difficult because of the following challenges:

- Friction is unknown or unmeasurable;
- Friction is neither constant nor evenly distributed;
- Friction is a nonlinear w.r.t. bristle deflection, motor speed and viscous force [2].

Therefore, linear controllers like PID are not suitable for the motion control of X/Y stages with $\mu$m-level precision. Actually, the DVM6 with DC motors performs much worse in stage speed and position accuracy than its main competitor VHX-6000 from Keyence with stepper motors.

If regarding the friction as disturbance, sliding mode control (SMC) can be used here with the benefits of [3]:

- Simplicity in application;
- Independence of matched disturbance;
- Order reduction by constraint of the system motion in a manifolder;
- No prior knowledge of system or disturbance is required to know, except the upper bound.

To alleviating the chattering [4] caused by SMC, a commonly used solution is the boundary layer design [5], where a smooth continuous function (saturator) is used to approximate the discontinuous sign function in a region called the boundary layer around the sliding surface, but sacrifice of position accuracy has to be paid. Recent research progress of chattering suppression mainly has two directions. One is to introduce integrator in SMC so that discontinuous function after integral becomes continuous [6]–[8]. The other is to increase the order of SMC [9], based on which super twisting algorithm is proposed and combined with adaptive change of control gain [10]. Both methods increase the complexity of controller implementation and the real-time computation burden of micro-controller unit (MCU). Consequently, cost increase is inevitable.

This paper aims to propose an low-cost way to implement $\mu$m-level precision for X/Y stage movement with DC motors and friction engagement. The whole paper is organized as follows. Section II introduces hardware used in DVM6, based on which SMC is implemented in Section III to achieve $\pm 2$ $\mu$m precision without any chattering. Validation is presented in Section IV by comparing the stage performance of the proposed solution with Leica DVM6 and Keyence VHX-6000. Section V draws the conclusion.

## II. HARDWARE DESCRIPTION OF THE STAGE

Fig. 1 shows the stage of DVM6 for our study. A diagram is given in Fig. 2 to show how the friction is engaged between DC motors and moving tracks [11]. The DC motor is mounted on a bracket attached to a spring to keep motor in position during motor operation. Roller bearings and springs are used to maintain a constant force exerted on the motor shaft against the parallel rod. Since DC motors are fixed to the X/Y stages,
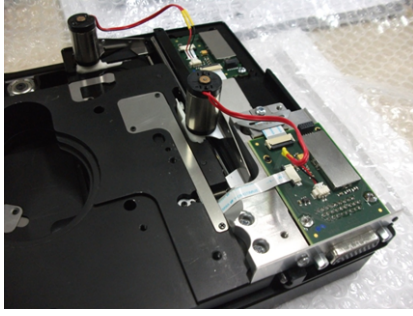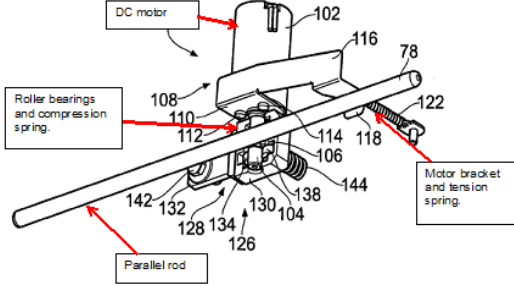
Fig. 1. Stage from Renishaw



Fig. 2. Diagram of friction engagement between DC motor and tracks

motor shaft moving along the rod (track) will pull the stage to move as well.
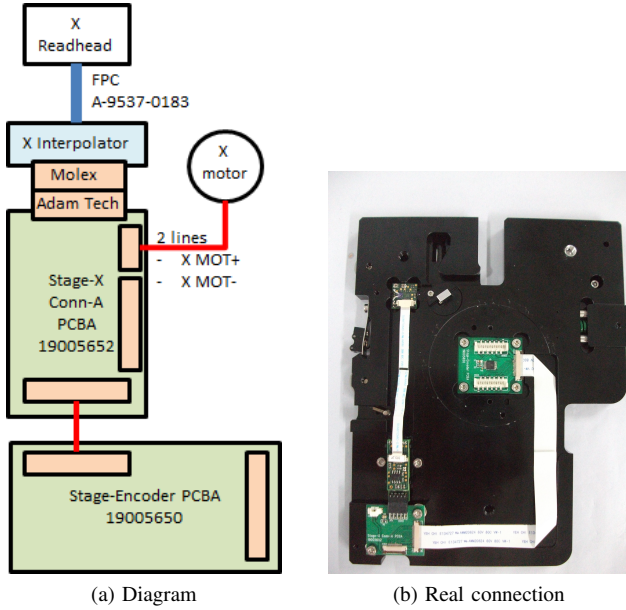


(a) Diagram      (b) Real connection

Fig. 3. Optical encoder for position

Optical scale/readhead from Renishaw gives the position encoder with the resolution of 0.2 $\mu$m, as shown in Fig. 3. Interpolator is used to digitalize the analog signal from the readhead. PCBA attached to the stage is in charge of the communication among encoder, motor and MCU.

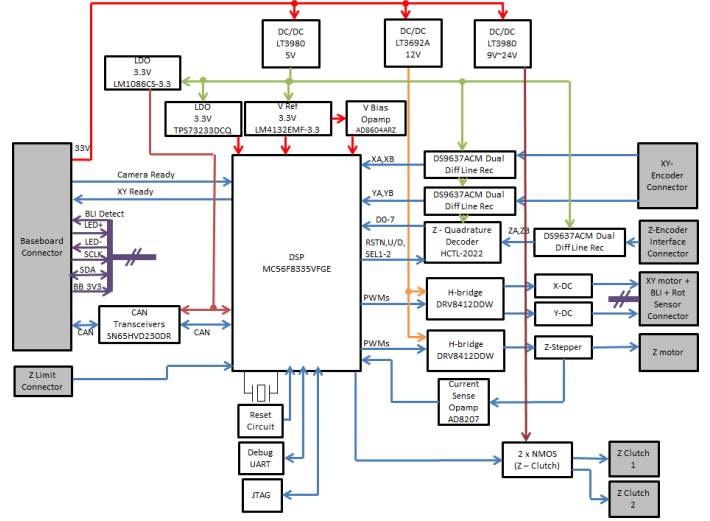Coreless DC motor from Namiki is used due to the size



Fig. 4. Connection of MCU with other components of microscopy

and weight constraints. MC56F8335 from Freescale is used as the MCU for our proposed motion control. The connection of MCU with other components of microscopy is shown in Fig. 4. Note that such an MCU is very old (launched in 2007 with 16-bit, 60 MHz maximum core frequency and no floating point support), it is a good platform to check if the proposed SMC increases the burden of real-time computation of MCU.

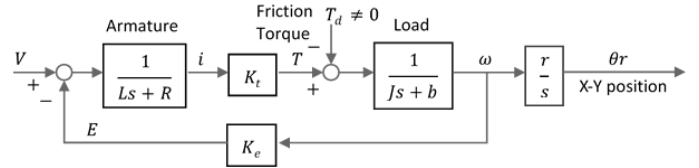## III. STAGE MOTION CONTROL WITH SMC



Fig. 5. Diagram of DC motor systems for DVM6

The system diagram of DC motors in DVM6 is shown in Fig. 5, where $V$ is input voltage; $E$ is back electro-motive force (EMF); $R$ and $L$ are armature resistance and inductance, respectively; $K_e$ is back EMF constant; $K_t$ is torque constant; $T$ and $T_d$ are torque from motor and friction, respectively; $J$ is rotor inertia; $b$ is viscous friction constant; $\omega$ is angular velocity; $\theta$ is rotation angle; and $r$ is the radius from rotor axis to the contact point on tracks, as shown in TABLE I.

TABLE I
SYSTEM VARIABLES

| Symbol | Value | Unit | Symbol | Value | Unit |
|--------|-------|------|--------|-------|------|
| $L$ | 0.16 | mH | $R$ | 11 | $\Omega$ |
| $K_t$ | 12.7 | mNm/A | $K_e$ | 1.3 | mV/rpm |
| $J$ | 1.1 | gcm$^2$ | $r$ | 1.542 | mm |

For coreless DC motors, $b \approx 0$. Since the electrical time constant $\tau_e = L/R = 14.5$ $\mu$s, which is much less than the
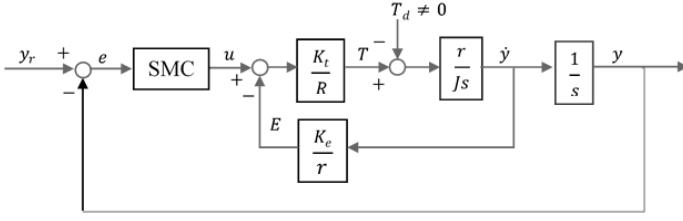
Fig. 6. Simplified motion control system with SMC



Fig. 7. System impulse response in case of friction

shortest sampling time of MCU (102 $\mu$s), dynamics in armature is undetectable in our control, i.e., $1/(Ls + R) \approx 1/R$. Hence, Fig. 5 can be further simplified as Fig. 6, where $r$ is put into the inner loop, $y$ and $y_r$ are the current and target position of the stage, respectively, and $e = y_r - y$ is the position error.

### A. Impact from Friction on System Dynamics

If $T_d = 0$, the transfer function from $u$ to $y$ is

$$G(s) = \frac{Y(s)}{U(s)} = \frac{1}{s(\tau s + 1)},$$

where $\tau = JR/(rK_t)$ is time constant. Its impulse response with $U(s) = K$ ($K > 0$ is constant) is given by

$$Y(s) = \frac{K}{s(\tau s + 1)} = K\left(\frac{1}{s} - \frac{\tau}{\tau s + 1}\right).$$

Converting to time domain yields

$$y(t) = K(1 - e^{-t/\tau}). \tag{1}$$

To show the impacts from friction on system dynamics, an impulse input is injected to the DC motor voltage and lasts for one cycle only, i.e.,

$$u(t) = \begin{cases} 12 \text{ V}, & 0 < t < T_s; \\ 0 \text{ V}, & \text{otherwise}. \end{cases}$$

Note that 12 V is the maximum voltage allowed for DC motor input, and $T_s = 102$ $\mu$s is the fastest sampling time allowed for the MCU. The real $y(t)$ corresponding to $u(t)$ above is shown in Fig. 7 with dotted blue line, whereas the simulated $y(t)$ given by (1) is presented by read line. It is clearly to see that friction causes damping up to 12 $\mu$m, which is significantly larger than the precision requirement of $\pm 2$ $\mu$m. Moreover, steady state value is greatly reduced from 150 $\mu$m to 6 $\mu$m (96% less). This simple test shows that the presence of friction fundamentally change the whole system.

### B. Friction Modelling

For all the modelling of friction, LuGre model is the most accepted one with the good balance between accuracy and ease of analysis. LuGre model is described by [12]

$$\frac{dz}{dt} = v - \sigma_0 \frac{|v|}{g(v)}z, \tag{2}$$
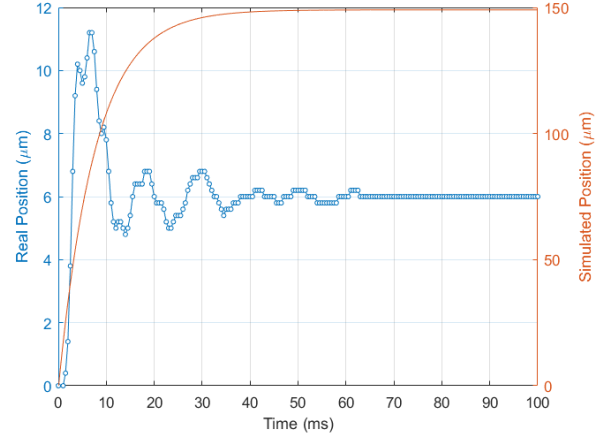
$$F = \sigma_0 z + \sigma_1 \dot{z} + f(v), \tag{3}$$

where $v$ is the velocity between the two surfaces in contact, $z$ is the internal friction state, and $F$ is the predicted friction force. Compared with the Dahl model [13], the LuGre model has a velocity-dependent function $g(v)$ instead of a constant, an additional damping $\sigma_1$ associated with microdisplacement, and a general form $f(v)$ for the memoryless velocity-dependent term. The state $z$, which is analogous to the strain in the Dahl model, can be interpreted as the average bristle deflection. The LuGre model reproduces spring-like behavior for small displacements, where the parameter $\sigma_0$ is the stiffness, $\sigma_1$ is the micro damping, and $f(v)$ represents viscous friction. A reasonable choice of $g(v)$ giving a good approximation of the Stribeck effect is

$$g(v) = F_c + (F_s - F_c)e^{-|v/v_s|^\alpha}, \tag{4}$$

where $F_s$ corresponds to the stiction force, and $F_c$ is the Coulomb friction force. $v_s$ determines how quickly $g(v)$ approaches $F_c$, and $\alpha \in [0.5, 2]$ is some constant. From (2)-(4), one sees clearly that $F$ is highly nonlinear to $v$. Since $T_d = F \times r$, the whole control system presented by Fig. 6 is not linear any more. To design a motion control to follow the speed profile strictly, PID is not capable.

### C. SMC Design

Let $x_1 = y$ and $x_2 = \dot{x}_1 = \dot{y}$, it derives from Fig. 6 that

$$\dot{x}_1 = x_2,$$
$$\dot{x}_2 = \left[\left(u - \frac{K_e}{r}x_2\right)\frac{K_t}{R} - T_d\right]\frac{r}{J}.$$

Let $e_1 = e = y_r - y$ and $e_2 = \dot{e}_1$, then $x_1 = y = y_r - e_1$ and $x_2 = \dot{x}_1 = \dot{y}_r - e_2$. Replacing state variables $x_1$ and $x_2$ with $e_1$ and $e_2$ gives

$$\dot{e}_1 = e_2, \tag{5}$$
$$\dot{e}_2 = \ddot{y}_r + \frac{K_e K_t}{JR}\dot{y}_r - \frac{K_e K_t}{JR}e_2 - \frac{rK_t}{JR}u + \frac{r}{J}T_d. \tag{6}$$

Define the sliding surface $\sigma = p_1 e_1 + p_2 e_2$ with $p_{1,2} > 0$, it follows from (5) and (6) that

$$\dot{\sigma} = p_2\left(\ddot{y}_r + \frac{K_e K_t}{JR}\dot{y}_r\right) + \left(p_1 - p_2\frac{K_e K_t}{JR}\right)e_2$$
$$- p_2\frac{rK_t}{JR}u + p_2\frac{r}{J}T_d. \tag{7}$$

If Friction is bounded, i.e., $0 < |T_d| \le T_m$, the SMC is given by

$$u = \frac{JR}{rK_t}\left[\left(\ddot{y}_r + \frac{K_e K_t}{JR}\dot{y}_r\right)\right.$$
$$\left. + \left(\frac{p_1}{p_2} - \frac{K_e K_t}{JR}\right)e_2 + \frac{\mu}{p_2}\mathrm{sgn}(\sigma)\right], \tag{8}$$

where $\mu > T_m p_2 r / J$. Substituting (8) into (7) yields

$$\dot{\sigma} = -\left[\mu\mathrm{sgn}(\sigma) - p_2\frac{r}{J}T_d\right]. \tag{9}$$

The proof of $e_{1,2} \to 0$ as $t \to \infty$ in (5) and (6) with SMC by (8) is given as follows. Choose Lyapunov function $V = \sigma^2/2 \ge 0$, it follows from (9) that

$$\dot{V} = \sigma\dot{\sigma} = -\left(\mu|\sigma| - p_2\frac{r}{J}T_d\sigma\right)$$
$$< -\left(p_2\frac{r}{J}T_m|\sigma| - p_2\frac{r}{J}T_d\sigma\right)$$
$$\le -p_2\frac{r}{J}\left(|T_d||\sigma| - T_d\sigma\right)$$
$$\le 0.$$

According to Lyapunov stability theorem, $\sigma \to 0$ as $t \to \infty$.

### D. Chattering Suppression

SMC given in (8) will definitely bring an undesirable chattering to DC motor's input because of the following factors:

- Estimation of $e_2$;
- Estimation of $\mu$;
- Discontinuity of sgn function.

Correspondingly, the chattering suppression design is also from the above aspects.

*1) Estimation of $e_2$:* Only position sensor is available for X/Y stage of microscopy, i.e., $e_1$ is directly measured. To get $e_2$, differentiation has to be done on $e_1$, which will also magnify the measurement error in $e_1$ especially for fast sampling system. Let

$$\frac{p_1}{p_2} - \frac{K_e K_t}{JR} = 0,$$

thus SMC in (8) doesn't contain any terms of $e_2$, which means no need to do estimation of $e_2$ anymore.

*2) Estimation of $\mu$:* $\mu$ is mainly affected by $T_m$, which can be assumed as a very large value based on the hardware constraints. But most of time, such a big $T_m$ is unnecessary for most of our working conditions. Note that $T_d$ mainly increases with the motor speed, the more realistic way to find a smaller $\mu$ is to limit the motor speed by following a special speed profile. This is also the requirements of motion control to improve the user experience. Fig. 8 shows the commonly used speed
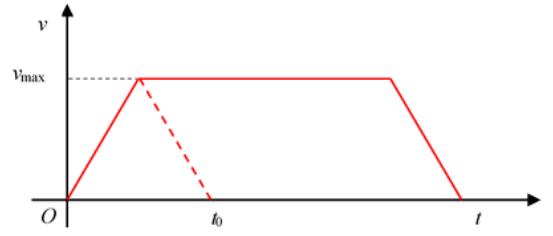


Fig. 8. Motor speed profile

profile for motion control. If $e(0) \le \int_0^{t_0} v\mathrm{d}t$, the speed profile is triangle. Otherwise, the speed profile is trapezoid. From (2)-(4), it is not difficult to derive that

$$\mu = T_m = (|g(v_m)| + |f(v_m)|) \times r.$$

*3) Discontinuity of sgn Function:* Boundary layer method is used to replace the discontinuous sgn($\cdot$) function with the continuous saturator function sat($\cdot$), as shown in Fig. 9. $d$ is a tuning parameter to get the balance between the accuracy and performance requirements.


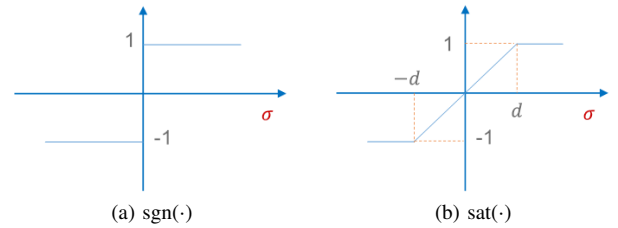
(a) sgn($\cdot$)    (b) sat($\cdot$)

Fig. 9. Boundary layer method

### E. Position Finetune

As aforementioned, chattering suppression of boundary layer method is with the sacrifice of accuracy loss. To fully compensate it, the following fine-tune algorithm is proposed, whose flowchart is shown in Fig. 10.

Step1. Check the steady state error $e$ of X/Y stage after settling down;

Step2. If $|e| > 2$ $\mu$m (10 count), adjust target position by $y_r^* = y_r e$;

Step3. Count the loop number $n$ for Step 1-2 and go back to Step 1;

Step4. Stop until $|e| \le 2$ $\mu$m (10 count) or the loop number $n \ge 3$.

Its effectiveness will be shown by the real test in the following section.

## IV. VALIDATION

To validate if the proposed SMC can achieve $\pm 2$ $\mu$m precision of stage movement, the following test procedure is designed:

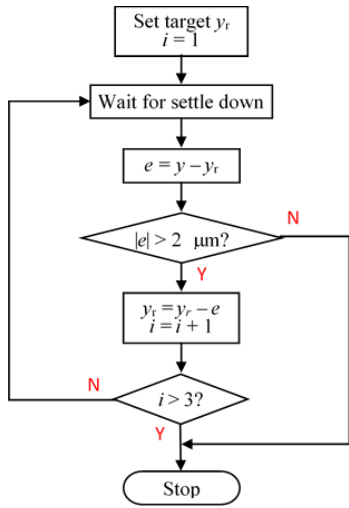Step1. Set zero point for X/Y stage movement and move the stage to zero;

Fig. 10. Finetune algorithm

Step2. Towards positive direction, move X/Y stage with the step size of 80 $\mu$m (400 counts) until the stage reaches 20 mm (100,000 counts);

Step3. Towards negative direction, move X/Y stage with the step size of 80 $\mu$m (400 counts) until the stage reaches -20 mm (-100,000 counts);

Step4. Towards positive direction, move X/Y stage with the step size of 80 $\mu$m (400 counts) until the stage reaches zero;

Step5. Repeat Step 2-4 with multiple ($2\times$, $3\times$, , $250\times$) step size of 80 $\mu$m,
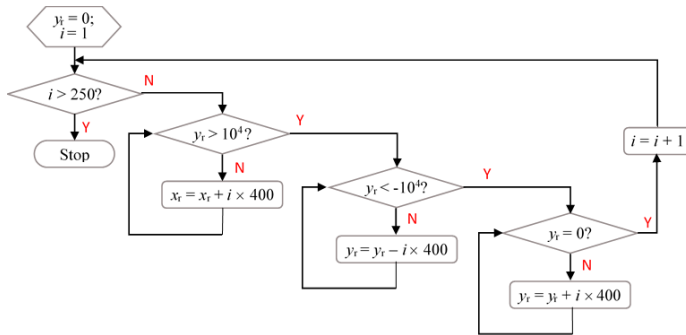
and the flowchart is shown in Fig. 11.



Fig. 11. Test procedures

SMC parameters are chosen to be $\mu = 8.66$ V and $d = 20$ $\mu$m, and the statistics of the test results are shown in TABLE II and Fig. 12, respectively. Of the total 5684 target positions, SMC with the fine-tune algorithm achieves 100% rate for the position errors within the tolerance of $\pm 2$ $\mu$m. Histogram plots shows how the Gaussian distribution of position errors is squeezed to meet the precision requirements by the fine-tune algorithm.

## A. Comparison with PID

To show the differences of SMC and PID in their capability of speed profile following, we let the X stage move from 0 to 20 mm by following the same speed profile as shown in Fig. 8. The results are shown in Fig. 13, and it is clear to see that SMC can strictly follow the predefined speed profile, whereas PID cannot.

More quantitative comparison is done by measuring the time of tile scan with different settings of zoom values, FOV and scan areas. To compare fairly, resolution of $1600 \times 1200$ pixel, exposure time of 5 ms and gain of 1.0 are in common. Three cases of different test settings are listed in TABLE III together with the scan time for PID and SMC. For all cases, SMC achieves at least 33% faster in stage movement than PID.

## B. Comparison with Stepper Motors

A similar tile scan test is also done on Keyence VHX-6000 with stepper motors to compare with the proposed SMC with DC motors. The results are shown in TABLE IV. Since the test is done on a real microscopy, the scan time is also affected by the speed of camera, not depends on stage performance only. Nevertheless, the proposed solution can still catch up the best performance of stepper motor.

## V. CONCLUSION

A low-cost precision motion control for X/Y stage of microscopy is proposed and fully analyzed. Challenges in control are highlighted in case of friction is engaged between motor shaft and stage tracks. Instead of using stepper motors, the proposed motion control uses DC motors only but needs SMC to strictly follow the speed profile. Boundary layer method are used to suppress the chattering as normal, but a simple trick of position fine tune is proposed to fully compensate the accuracy loss. The effectiveness of the proposed method is proved by comparison with PID control. Comparison with Keyence VHX-6000 (which uses stepper motors for their stages) shows that the proposed solution achieves the similar performance but the cost is much lower.

## REFERENCES

[1] D. R. McMurtry and I. S. Bennell, "Sample positioning stage and method of operation," U.S. Patent 8 254 002 B2, Jul. 17, 2008.

[2] H. Olsson, K. J. Åström, C. C. de Wit, M. Gäfvert, and P. Lischinsky, "Friction models and friction compensation," *European Journal of Control*, vol. 4, no. 3, pp. 176 – 195, 1998. [Online]. Available: http://www.sciencedirect.com/science/article/pii/S094735809870113X

[3] A. Sabanovic, "Variable structure systems with sliding modes in motion control—A survey," *IEEE Transactions on Industrial Informatics*, vol. 7, no. 2, pp. 212–223, May 2011.

[4] V. Utkin and H. Lee, "Chattering problem in sliding mode control systems," in *International Workshop on Variable Structure Systems, 2006. VSS'06.*, June 2006, pp. 346–350.

[5] J. A. BURTON and A. S. I. ZINOBER, "Continuous approximation of variable structure control," *International Journal of Systems Science*, vol. 17, no. 6, pp. 875–885, 1986. [Online]. Available: http://dx.doi.org/10.1080/00207728608926853

[6] M.-L. Tseng and M.-S. Chen, "Chattering reduction of sliding mode control by low-pass filtering the control signal," *Asian Journal of Control*, vol. 12, no. 3, pp. 392–398, 2010. [Online]. Available: http://dx.doi.org/10.1002/asjc.195

TABLE II
TEST RESULTS

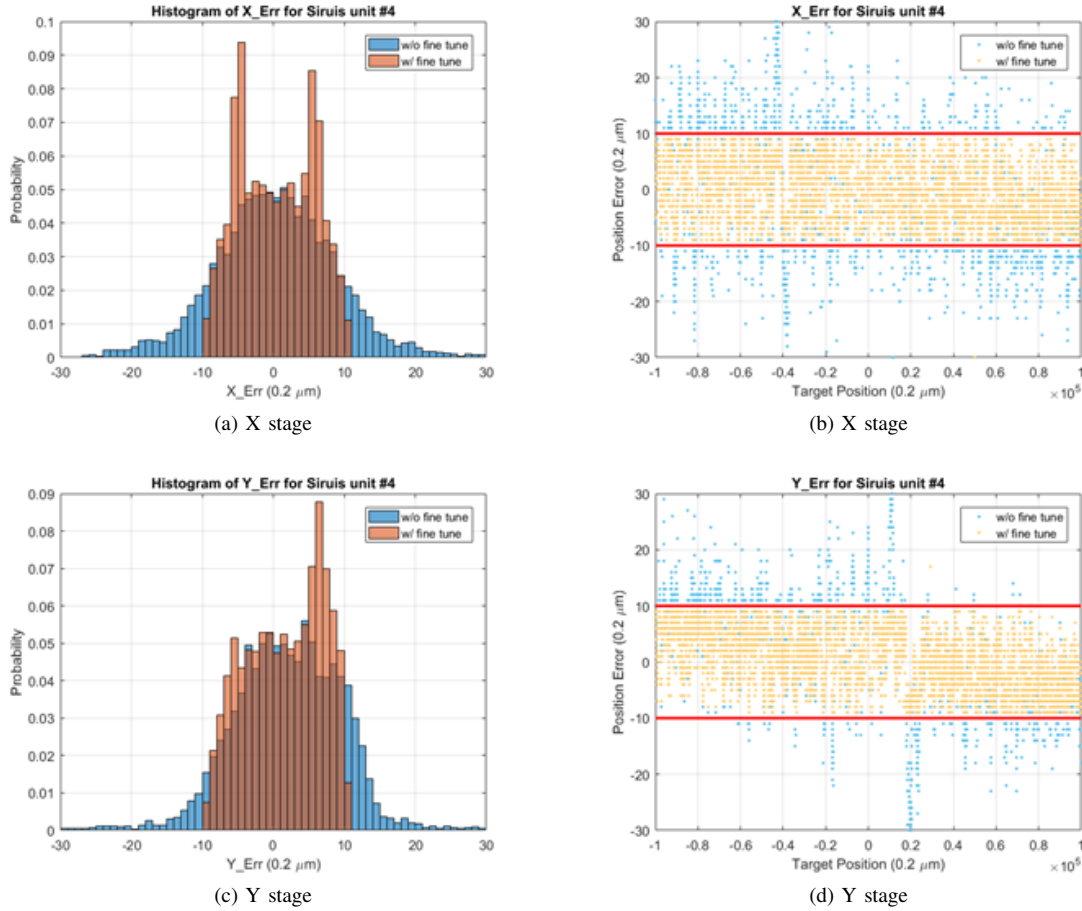| Total Positions | Stage | Fine-tuned? | Mean (μm) | Std (μm) | No. within ±2 μm | % within ±2 μm |
|---|---|---|---|---|---|---|
| 5684 | X | No | -0.0331 | 1.7486 | 4605 | 81.02% |
| | | Yes | -0.0217 | 1.0553 | 5684 | 100% |
| | Y | No | 0.2947 | 1.5438 | 4856 | 85.43% |
| | | Yes | 0.2153 | 1.1228 | 5684 | 100% |



(a) X stage

(b) X stage

(c) Y stage

(d) Y stage

Fig. 12. Histogram of position errors before and after fine-tune

TABLE III
TILE SCAN CASES

| Case | Zoom | FOV X×Y | Scan Area | PID | Proposed |
|---|---|---|---|---|---|
| I | 10× | 1mm×0.75mm | 10mm×7.5mm | 98s | 51s |
| II | 5× | 2mm×1.5mm | 20mm×15mm | 96s | 58s |
| III | 2× | 5mm×3.75mm | 50mm×37.5mm | 100s | 67s |

TABLE IV
TILE SCAN CASES

| Zoom | FOV X×Y | Scan Area | VHX-6000 | Proposed |
|---|---|---|---|---|
| 2.93× | 3.4mm×2.5mm | 14mm×15mm | 31s | 37s |

[7] J. X. Xu and K. Abidi, "Discrete-time output integral sliding-mode control for a piezomotor-driven linear motion stage," *IEEE Transactions on Industrial Electronics*, vol. 55, no. 11, pp. 3917–3926, Nov 2008.

[8] K. Abidi, J. X. Xu, and Y. Xinghuo, "On the discrete-time integral sliding-mode control," *IEEE Transactions on Automatic Control*, vol. 52, no. 4, pp. 709–715, April 2007.

[9] G. Bartolini, A. Ferrara, E. Usai, and V. I. Utkin, "On multi-input chattering-free second-order sliding mode control," *IEEE Transactions on Automatic Control*, vol. 45, no. 9, pp. 1711–1717, Sep 2000.

[10] V. I. Utkin and A. S. Poznyak, "Adaptive sliding mode control with application to super-twist algorithm: Equivalent control method," *Automatica*, vol. 49, no. 1, pp. 39 – 47, 2013. [Online]. Available: http://www.sciencedirect.com/science/article/pii/S0005109812004694

[11] V. Stimpson, B. Smith, A. Woolfrey, and M. Hill, "Sample positioning apparatus," U.S. Patent 0 310 215 A1, Jun. 30, 2009.

[12] K. J. Åström and C. C. de Wit, "Revisiting the lugre friction model," *IEEE Control Systems Magazine*, vol. 28, no. 6, pp. 101–114, 2008.

[13] P. Dahl, "A solid friction model," The Aerospace Corporation, El Segundo, CA, Technical Report TOR-0158(3107-18)-1, 1968.
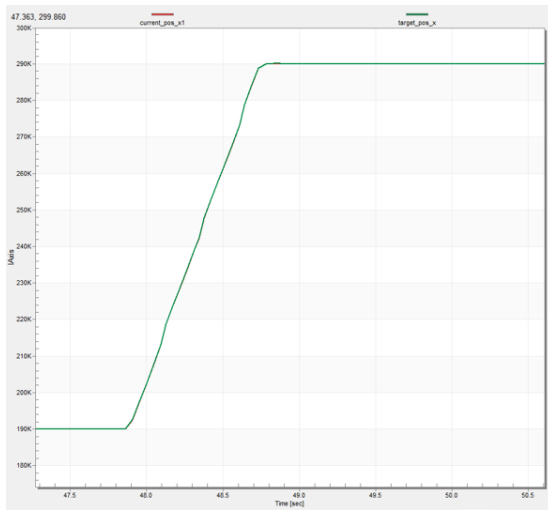
(a) SMC
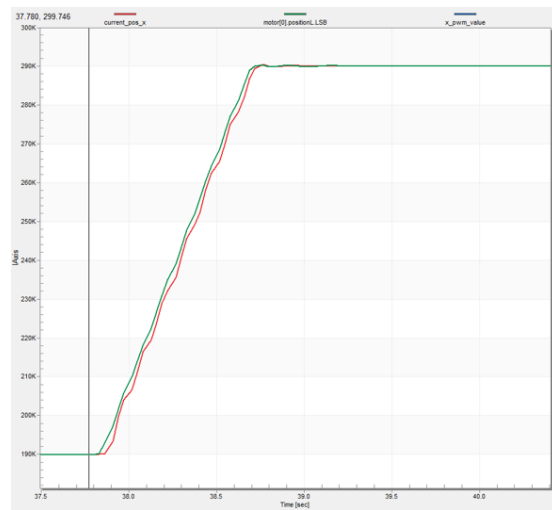
(b) PID

Fig. 13. Comparison between SMC and PID in speed profile following